b-Hadron Spectroscopy

M. MOCH

IEKP, University of Karlsruhe,
D-76128 Karlsruhe, Germany
E-mail: moch@ekp.physik.uni-karlsruhe.de

Abstract

The theoretical expectations and the current experimental status of orbitally excited B-mesons and of $\Sigma_b^{(*)}$-baryons are reviewed. Preliminary new analyses of $B_{u,d}^{**}$-, B_s^{**}-mesons and $\Sigma_b^{(*)}$-baryons from the DELPHI Collaboration are presented.

1 Introduction

B-mesons are very well suited to study the QCD potential since they correspond to the hydrogen atom due to the large mass of the b-quark. This leads to a decoupling of the b-quark's spin S_b and the total angular momentum of the light quark j_q. For an orbital momentum of $L = 1$ this results in two doublets with $j_q = 1/2, 3/2$. These four states are commonly termed B**. Their properties are summarised in table 1 for the case that the light quark is a u- or a d-quark. For B_s^{**}-mesons the same properties and behaviour are expected but the main decay should be the decay $B_s^{**} \to B^{(*)}K$ if the mass is above the BK threshold since the decay into $B_s^{(*)}\pi^0$ is forbidden by isospin conservation.

579

J^P	$B_{u,d}^{**}$-State	Main Decay Mode	Transition
0^+	B_0^*	$B\pi$	S-wave (broad)
1^+	B_1^*	$B^*\pi$	S-wave (broad)
1^+	B_1	$B^*\pi$	D-wave (narrow)
2^+	B_2^*	$B^*\pi, B\pi$	D-wave (narrow)

Table 1: Properties of $B_{u,d}^{**}$-mesons.

2 Theoretical Expectations

The decoupling of the light degrees of freedom and the spin of the b-quark results in symmetries concerning the flavour of the heavy quark (c- or b-quark) and its spin, leading to an effective theory of QCD, the Heavy Quark Effective Theory (HQET) [1, 2]. Thus, experimental results from the charm sector (see table 2) can be used to predict the mass splittings within a doublet by scaling the spittings for D**-mesons by the ratio of c-quark and b-quark mass m_c/m_b. This gives an excellent agreement for the splitting within the ground state doublet (B*,B) and leads to a prediction of 12 MeV for the splitting within the narrow doublet $m(B_2^*) - m(B_1)$ and of approximately 45 MeV for the splitting within the broad doublet $m(B_1^*) - m(B_0^*)$.

However, for the splitting between the two doublets HQET is not applicable. Models have to be used for this. There are two classes of such models: The first one predicting that the narrow states lie lower in mass than the broad ones (so-called spin-orbit inversion) [3, 4] and the second one predicting that the narrow states lie higher in mass than the broad ones [5]. The latter seems to be favoured by the D** results but this must not necessarily be valid for B**, too. The widths of the broad states are expected to be equal and to lie in the range [200,300] MeV [4, 6].

3 Experimental Status of $B^{**}_{u,d}$

Evidence for the existence of narrow $B^{**}_{u,d}$-states first emerged in analyses at LEP in which a charged pion produced at the primary event vertex was combined with an inclusively reconstructed B-meson [10]-[12]. In a subsequent analysis, the ALEPH Collaboration performed an analysis combining a primary charged pion with a fully reconstructed B-meson [13] and measured the mass and rate in a fit to the mass spectrum with fixed mass differences, widths and relative rates of all spin states according to the predictions of [14]. Subsequently the L3 Collaboration presented an inclusive measurement of the mass and width of the B^*_1- and B^*_2-states by a fit imposing constraints that reflect the level of understanding regarding the widths and masses of the B^{**}-states circa 1999 [15]. More recently, the CDF Collaboration have presented the first results on $B^{**}_{u,d}$-production from a hadron collider [16] by combining a charged primary pion to a partially reconstructed B using semileptonic decays to charm.

Table 3 summarises these measurements for the $B^{**}_{u,d}$-states. In order to make a comparison possible, published numbers have been adjusted where possible to be valid for a common set of input parameters, e.g. $B_{u,d}$ production fractions [17].

4 Motivation

Until now it has not been possible to separate the contributions of the four states to the signal observed. Thus, the mass hierarchy of the B^{**}-mesons is not clear and the corresponding production rates as well. This is an experimental topic since the predictions are very model dependent. To be able to separate the contribution of the broad states it is necessary to reduce the uncertainty on the background. This has been achieved in two ways: The first one, the High Efficiency Approach (HEA), is a conventional, cut-based analysis in which the dependence on the Monte Carlo model is reduced by ana-
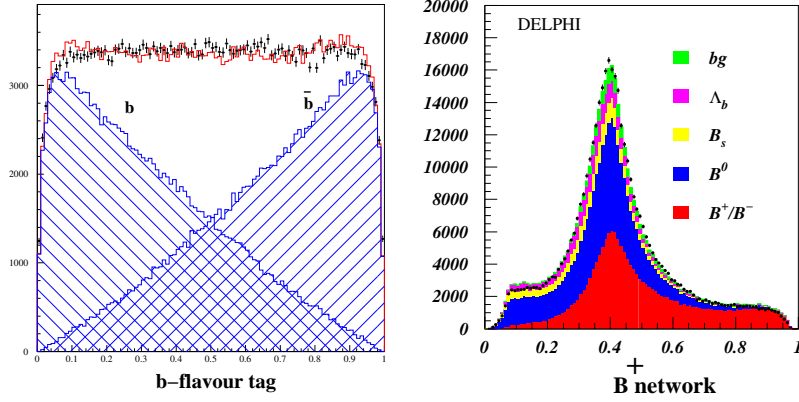
Figure 1: Separation of b- and b̄-quarks in the HEA (left) and the output of the B^+ identification network in the HPA (right).

lytically parametrising the background shape and fitting it to data. The second one, the High Purity Approach, targets the best achievable signal-to-background ratio by using neural networks to perform B-momentum reconstruction, identification of the weakly decaying b-hadron and B^{**} enrichment.

In the following the measured quantity which is denoted "rate" is the fraction of the state considered per b-jet, e.g.:

$$\frac{\sigma(B^{**}) \cdot \mathrm{BR}(B^{**} \to B^{(*)}\pi)}{\sigma_b}$$

The variable reconstructed in the analyses is the Q-value of the B^{**} decay defined as:

$$Q \quad = \quad m(\mathrm{B}^{(*)}\pi) - m(\mathrm{B}) - m(\pi) \qquad (1)$$

582

where $m(\mathrm{B}^{(*)}\pi)$ denotes the invariant mass of the $\mathrm{B}\pi$ system[1] and $m(\mathrm{B})$ and $m(\pi)$ are the B- and pion mass respectively.

Since only charged tracks are considered in the analyses the measured rates are scaled by an isospin factor to account for unseen decays into neutral pions and kaons. This factor is 1.5 for $\mathrm{B}^{**}_{u,d}$ and $\Sigma^{(*)}_b$ and 2.0 for B^{**}_s.

5 $\mathrm{B}^{**}_{u,d}$-Mesons

The decays considered in the analyses presented in this section are

$$\begin{aligned}
\mathrm{B}^{**}_u(\bar{b}u) &\longrightarrow \mathrm{B}^0\pi^+ \\
\mathrm{B}^{**}_d(\bar{b}d) &\longrightarrow \mathrm{B}^+\pi^-
\end{aligned} \tag{2}$$

The correlation between the charge of the pion and the charge of the b-quark inside the B^{**}-meson and the inclusive reconstruction of B^+- and B^0-mesons are very important for both approaches. The separation power of the HEA b-flavour tag is illustrated in figure 1 on the left. The output of the network used in HPA to enrich B^+-mesons is shown in the same figure on the right. The decay pion which originates from the primary vertex has to be separated from fragmentation tracks in order to enrich B^{**}-mesons. The correlations mentioned above are used to define a right sign and a wrong sign sample and $\mathrm{B}^{**}_u/\mathrm{B}^{**}_d$ samples respectively.

In the High Efficiency Analysis, the signal has been described by a Gaussian. Additionally, a Breit-Wigner has been introduced to describe a shoulder at a Q-value of about 500 MeV. The right-sign samples for B^{**}_u and B^{**}_d have been combined to form just a B^{**} sample. The same has been done with the wrong-sign samples. A

---

[1]Note that B*-mesons are not reconstructed. Thus, a B** decaying into B*π appears about 46 MeV lower in the reconstructed Q-spectrum.
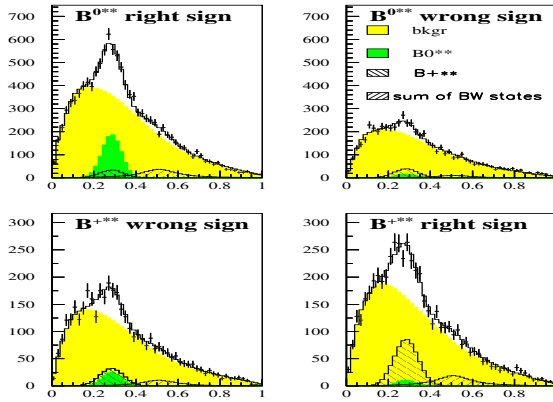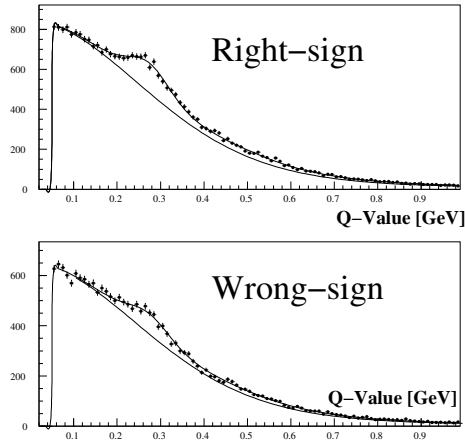
Figure 2: Fit result of the HEA for $B^{**}_{u,d}$ (upper). The fitted background is superimposed. Combined fit result of the HPA for $B^{**}_{u,d}$ (lower).

584

simultaneous fit to the right- and wrong-sign Q-value distributions has been performed ($\chi^2/d.o.f. = 0.9$) giving a rate of

$$\frac{\sigma(B^{**}) \cdot \mathrm{BR}(B^{**} \to B^{(*)}\pi)}{\sigma_b} = 0.122 \pm 0.014(\mathrm{stat}) \pm 0.018(\mathrm{syst}) \quad (3)$$

at a mean Q-value of $Q = 292 \pm 3 \pm 12$ MeV with a width of $\sigma = 45 \pm 4 \pm 4$ MeV. The fit to the Q-distribution is shown in figure 2 on the left.

The working point for the High Purity Analysis has been chosen at a higher B^{**} purity. All four Q-spectra for the B_d^{**} right-sign and wrong-sign sample and for the B_u^{**} samples have simultaneously been fitted with the constraint that the rate for B_d^{**} is equal to the one of B_u^{**}. The background shape has been taken from Monte Carlo and has been corrected by a cubic polynomial in Q whose parameters have been left free in the fit. The signal has been described by two Gaussians with the same mean but different widths for B_d^{**} and B_u^{**} respectively and an additional Breit-Wigner to take into account an excess observed at a Q-value of about 500 MeV. The fit ($\chi^2/d.o.f. = 1.0$) has resulted in a rate of

$$\frac{\sigma(B^{**}) \cdot \mathrm{BR}(B^{**} \to B^{(*)}\pi)}{\sigma_b} =$$
$$= 0.143 \pm 0.014(\mathrm{stat}) \pm 0.018(\mathrm{syst}) \quad (4)$$

at a mean Q-value of $Q = 286 \pm 3(\mathrm{stat}) \pm 12(\mathrm{syst})$ MeV with widths of $\sigma(B_d^{**}) = 46 \pm 5 \pm 3$ MeV and $\sigma(B_u^{**}) = 57 \pm 6 \pm 4$ MeV. The fit to the Q-distribution is shown in figure 2 in the middle and on the right.

One would expect up to three narrow peaks from the three main decays of the narrow B^{**} decays (see table 1). Monte Carlo studies have shown that these peaks are not resolvable. Thus, one expects one peak with a possibly broadened shape. Since the fitted widths are compatible with the expected resolutions the observed signal is

585
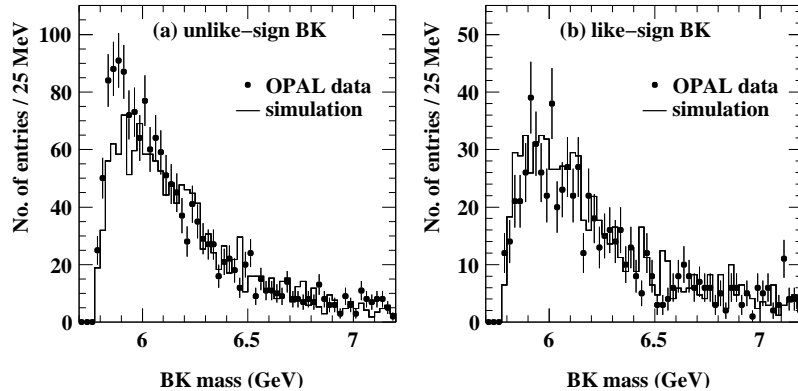
Figure 3: B_s^{**} result of the OPAL Collaboration.

interpreted as coming from narrow states. The Breit-Wigner component with a statistical significance of 2.5σ is not interpreted as broad B^{**}-states since the charm sector does not support the idea of spin-orbit inversion. Possible interpretations are radial or higher orbital excitations, a statistical fluctuation or an analysis artefact.

6 B_s^{**}-Mesons

The OPAL Collaboration was the first to observe an excess in the right-sign $B^{(*)}K$ spectrum in the range 5800-6000 MeV (see figure 3) giving a rate of

$$\frac{\sigma(B_s^{**}) \cdot \mathrm{BR}(B_s^{**} \to B^{(*)}K)}{\sigma_b} = 0.020 \pm 0.006 \qquad (5)$$

The DELPHI Collaboration has studied the decay $B_s^{**} \to B^+K^-$ within the framework of the High Purity Approach by replacing the decay pion by a kaon identified by a neural network combining the

586

information available from the TPC and the RICHes. Since all information has been used as input to the B_s^{**} enrichment network to obtain the best possible performance, a wrong-sign sample cannot be defined. Thus, the background has been parametrised by an analytical function. The observed Q-spectrum is shown in figure 4 on the left. The measured rate is

$$\frac{\sigma(B_s^{**}) \cdot \mathrm{BR}(B_s^{**} \to B^{(*)}K)}{\sigma_b} =$$
$$= 0.010 \pm 0.002(\mathrm{stat}) \pm 0.003(\mathrm{syst}) \quad (6)$$

at a Q-value of $Q = 76.3 \pm 3.2(\mathrm{stat}) \pm 4.7(\mathrm{syst})$ MeV. A similar analysis within the framework of the High Efficiency Approach has given an upper limit for the rate of < 0.015 @ 95% CL.

As for the B** analyses one would also expect here up to three peaks from the different decays of the narrow states. But only one peak can be seen. Since the Gaussian width of the signal observed is consistent with the expected detector resolution this peak is interpreted as originating from the decay of one narrow state. But how should this peak be interpreted and where is the second peak? The position of the second peak depends on the origin of the peak observed. There are two possible interpretations: The first is that it stems mainly from the decay of the B_{s1}-state. In this case one should clearly see a signal at a Q-value around 140 MeV for both scenarios of spin and state counting. The second assumes that the observed signal originates from the decay $B_{s2}^* \to BK$ in which case a clear signal is expected at a Q-value around 20 MeV. However, this signal might be smaller than expected due to the enhancement of the isospin forbidden decay $B_{s1} \to B_s^* \pi$ near threshold. This second interpretation constitutes the most likely explanation of the data.

587

$\Sigma_b^{+-(*)} \rightarrow \Lambda_b \pi^{+-}$
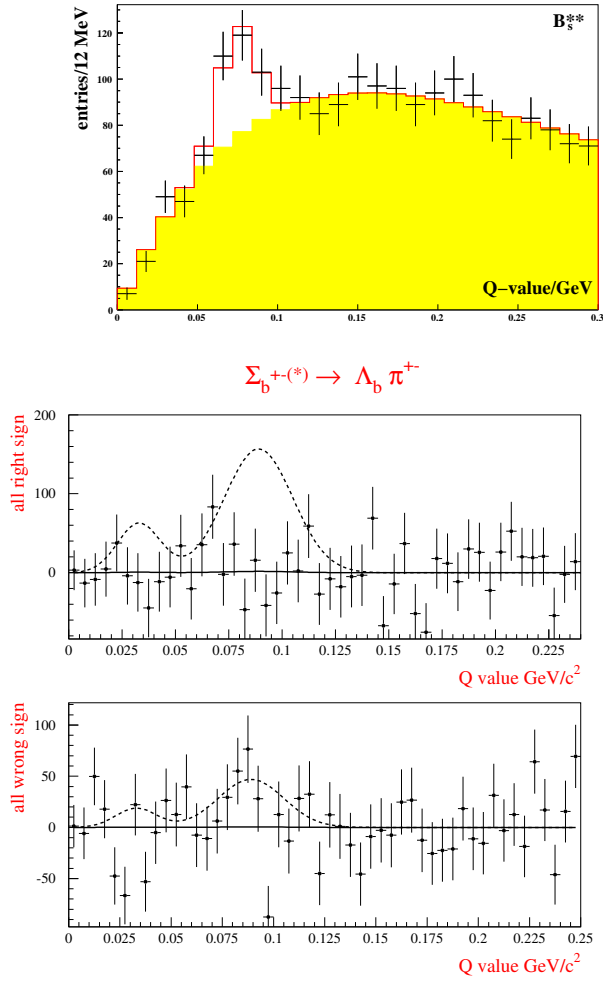
Figure 4: Fit result for B_s^{**} (left). $\Sigma_b^{(*)}$ spectra used for extracting the limit (right). The expected signal for a rate of 3% is superimposed.

7 $\Sigma_b^{(*)}$-Baryons

The b-baryons with an orbital angular momentum of zero are Λ_b, Σ_b and Σ_b^*. The expected decay mode for the Σ_b-baryon states is $\Sigma_b^{(*)} \to \Lambda_b \pi$. There are no published results for $\Sigma_b^{(*)}$-baryons yet but an old DELPHI conference result for the rate of $0.048 \pm 0.006 \pm 0.015$ was presented in 1995 [18]. A search for $\Sigma_b^{(*)}$-baryons has been performed by replacing the inclusively reconstructed B-meson by a Λ_b. No signal is observed. An upper limit on the production rate of a narrow resonance up to a $Q = 150$ MeV has been extracted:

$$\frac{\sigma(\Sigma_b^{(*)})}{\sigma_b} \quad < \quad 0.015 \text{ @ } 95\% \text{ CL.} \tag{7}$$

Thus, the previous DELPHI result is not confirmed. The background subtracted right-sign and wrong-sign Q-spectra used for extracting the limit are shown in figure 4 on the right. The expected signal for a production rate of 3%, i.e. the 1σ lower bound of the old DELPHI result, is superimposed.

8 Summary and Conclusions

Two complementary DELPHI analyses measure a narrow $B_{u,d}^{**}$ production rate per b-jet of:

A significant signal for one narrow B_s^{**}-state has been isolated by DELPHI at a Q-value of $Q = 76 \pm 3 \pm 5$ MeV giving a production rate per b-jet of

$$\frac{\sigma(B_s^{**}) \cdot \text{BR}(B_s^{**} \to B^{(*)}K)}{\sigma_b} \quad = \quad 0.010 \pm 0.002 \pm 0.003$$

For $\Sigma_b^{(*)}$, no signal could be observed. An upper limit on the production rate of a single resonance has been extracted:

$$\frac{\sigma(\Sigma_b^{(*)})}{\sigma_b} \quad < \quad 0.015 \text{ @ } 95\% \text{ CL.}$$

589

All results are preliminary.

References

[1] M. Voloshin and M. Shifman, Sov. J. Nucl. Phys. **45** (1987) 292 and **45** (1987) 292; N.Isgur and M. Wise, Phys. Lett. **B232** (1989) 113 and **B237** (1990) 527.

[2] B. Grinstein, Nucl. Phys **B339** (1990) 253; H. Georgi, Phys. Lett. **B240** (1990) 447; A. Falk, H. Georgi, B. Grinstein and M. Wise, Nucl. Phys. **B343** (1990) 1.

[3] D. Ebert, V. O. Galkin and R. N. Faustov, Phys. Rev. **D 57** (1998) 5663; Erratum-ibid. **D 59** (1999) 019902.

[4] N. Isgur, Phys. Rev. **D 57** (1998) 4041.

[5] M. Gronau and J. L. Rosner, Phys. Rev. **D49** (1994) 254; S. N. Gupta and J. M. Johnson, Phys. Rev. **D 51** (1995) 168.

[6] S. Godfrey and R. Kokoski, Phys. Rev. **D 43** (1991) 1679.

[7] BELLE Collab., K. Abe et al., BELLE-CONF-0235, submitted to ICHEP02.

[8] CLEO Collab., S. Anderson et al., Nucl. Phys. **A 663** (2000) 647.

[9] Particle Data Group, K. Hagiwara et al, Phys. Rev. **D 66** (2002) 010001.

[10] ALEPH Collab., D. Buskulic et al., Z. Phys. **C 69** (1996) 393;

[11] DELPHI Collab., P. Abreu et al., Phys. Lett. **B345** (1995) 598.

[12] OPAL Collab., R. Akers et al., Z. Phys. **C 66** (1995) 19.

590

[13] ALEPH Collab., R. Barate et al., Phys. Lett. **B 425** (1998) 215.

[14] E. Eichten, C. T. Hill and C. Quigg, Phys. Rev. Lett. **71** (1993) 4116;
E. Eichten, C. T. Hill and C. Quigg, Fermilab Conf 94/118 T.

[15] L3 Collab., M. Acciarri et al., Phys. Lett. **B465** (1999) 323.

[16] CDF Collab., T. Affolder et al., Phys. Rev. **D 64** (2001) 072002.

[17] Compiled by C. Weiser, 2002; updated for new numbers.

[18] DELPHI Collab., M. Feindt et al., EPS-HEP 95 Ref. eps0565.

	Meson	Mass [MeV]	Width [MeV]
BELLE [7]	D_0^{0*}	2308 ± 36	276 ± 66
BELLE [7]	D_1^{0*}	2427 ± 36	384 ± 117
CLEO [8]	D_1^{0*}	2461 ± 50	290 ± 100
World Av. [9]	D_1^0	2422.2 ± 1.8	$18.9^{+4.6}_{-3.5}$
World Av. [9]	D_2^0	2458.9 ± 2.0	23 ± 5
World Av. [9]	D_{sJ}^+	2572.4 ± 1.5	15^{+5}_{-4}
World Av. [9]	D_{s1}^+	2535.34 ± 0.31	< 2.3

Table 2: Current world results for the mass and the width of D^{**}-states.

	$m(B_{u,d}^{**})$ [MeV/c^2]	$\sigma(B_{u,d}^{**})/\sigma_b$
OPAL incl.	5712 ± 11	0.21 ± 0.05
DELPHI incl.	$5732 \pm 5 \pm 20$	$0.27 \pm 0.02 \pm 0.06$
ALEPH incl. (all)	$5734 \pm 3 \pm 16$	$0.214 \pm 0.012 \pm 0.045^{+0.030}_{-0.045}$
ALEPH incl.(peak)	$5734 \pm 3 \pm 16$	$0.144 \pm 0.008 \pm 0.030$
L3 incl.	$B_2^* : 5768 \pm 5 \pm 6$	$0.32 \pm 0.03 \pm 0.06$
CDF semi-excl.	$B_1 : 5710 \pm 20$	$0.22 \pm 0.05 \pm 0.02$
ALEPH excl.	$B_2^* : 5739^{+8+6}_{-11-4}$	$0.24 \pm 0.07^{+0.05}_{-0.04}$

Table 3: Current world results for masses and production rates of $B_{u,d}^{**}$-states.

	$\frac{\sigma(B_{u,d}^{**}) \cdot \mathrm{BR}(B_{u,d}^{**} \to B^{(*)}\pi)}{\sigma_b}$	$Q\left(B_{u,d}^{**}\right)$/MeV
'High Efficiency Approach'	$0.122 \pm 0.014 \pm 0.018$	$292 \pm 3 \pm 12$
'High Purity Approach'	$0.143 \pm 0.014 \pm 0.018$	$286 \pm 3 \pm 12$